Supplemental material

Dong et al., https://doi.org/10.1083/jcb.201802125

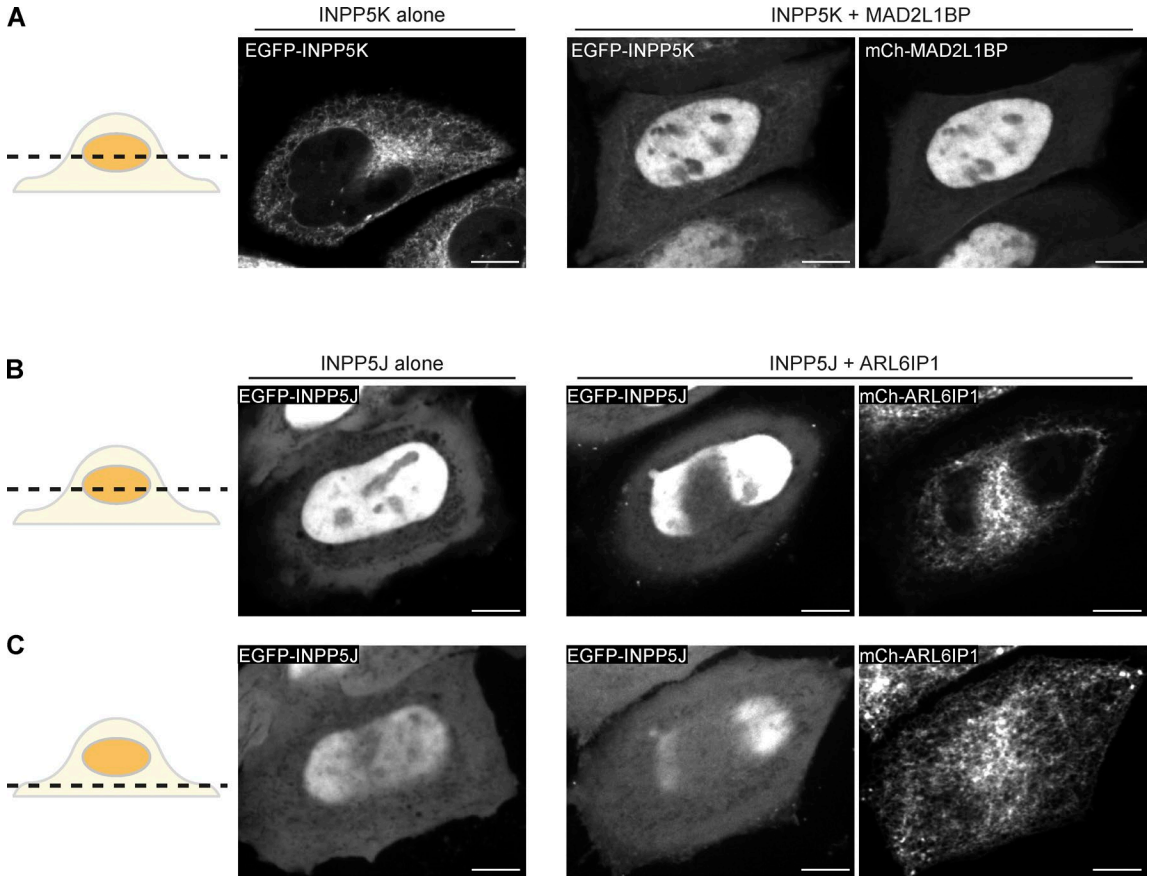

Figure S1. **Recruitment of INPP5K to the nucleus by MAD2L1BP and lack of INPP5J colocalization with ARL6IP1 on the ER. (A)** Recruitment of INPP5K to the nucleus by MAD2L1BP. Confocal images of HeLa cells expressing EGFP-INPP5K alone, or coexpressing EGFP-INPP5K with mCh-MAD2L1BP, showing the accumulation of EGFP-INPP5K into the nucleus upon mCh-MAD2L1BP overexpression. Scale bars: 10 µm. Representative examples of several cells imaged in at least three independent experiments are shown. All transfected cells exibited the phenotype shown. **(B and C)** INPP5J is concentrated in the nucleus and not on the ER visualized by mCh-ARL6IP1. Confocal images of the equatorial (B) or basal (C) focal planes (illustrations on the left) of HeLa cells expressing EGFP-INPP5J alone or coexpressing EGFP-INPP5J with mCh-ARL6IP1. The images show that EGFP-INPP5J is enriched in the nucleus but also localizes in the cytosol, and that the localization of EGFP-INPP5J is not affected by mCh-ARL6IP1 coexpression. Scale bars: 10 µm. Representative examples of several cells imaged in at least three independent experiments are shown. All transfected cells exhibited the phenotype shown.

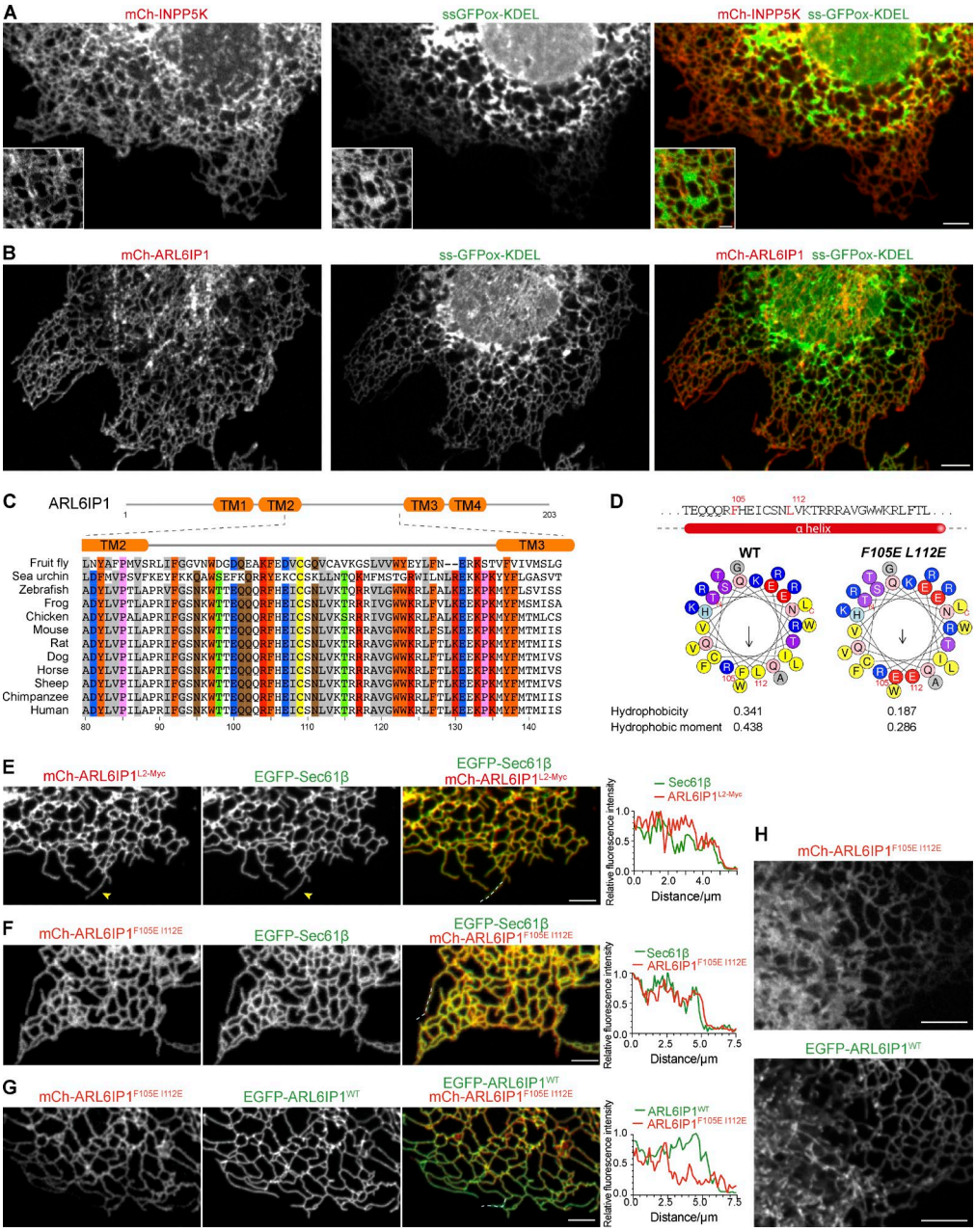

Figure S2. **Preferential localization of ARL6IP1 and INPP5K in peripheral ER tubules and role of a putaitve amphipatic helix in this localization. (A)** COS-7 cell coexpressing the ER luminal markers ss-GFPox-KDEL, mCh-INPP5K, and Myc-ARL6IP1 imaged by confocal fluorescence microscopy. Both ss-GFPox-KDEL and mCh-INPP5K fluorescence are present throughout the ER tubular network. However, mCh-INPP5K is enriched over ss-GFPox-KDEL in the peripheral tubular ER and is nearly undetectable in the nuclear envelope. Scale bar: 5 µm. Insets at the bottom left corners show the ER sheets of a different cell, demonstrating that mCh-INPP5K fluorescence is absent from the ER sheets marked by ss-GFPox-KDEL fluorescence. Inset scale bar: 2 µm. Images shown are representative of several cells imaged in more than three independent experiments. **(B)** Representative confocal images of a COS-7 cell coexpressing ss-GFPox-KDEL and mCh-ARL6IP1, showing the relative enrichment of mCh-ARL6IP1 over ss-GFPox-KDEL in the peripheral tubular ER and the presence of ss-GFPox-KDEL, but not mCh-ARL6IP1, on the nuclear envelope. Scale bar: 5 µm. **(C and D)** Sequence alignment of ARL6IP1 proteins from various species, focusing on their cytoplasm-facing portion between the second and third transmembrane regions (denoted as L2). The numbers of amino acids indicate those of human ARL6IP1. This stretch of amino acid is predicted to contain an α-helix with amphipathic properties, as represented by the helical wheel in left panel of D. Phenylalanine105 and leucine112 on the hydrophobic surface of the amphipathic helix were mutated to glutamic acid (F105E I112E) to disrupt its amphipathic property (right panel of D). Predictions were performed with the Heliquest server (http://heliquest.ipmc.cnrs.fr). **(E)** Representative confocal images and line-scan analysis of COS-7 cells coexpressing EGFP-Sec61β and mCh-tagged ARL6IP1 mutant whose L2 region was replaced with an amino acid flexible linker of equivalent length consisting of myc epitopes (mCh-ARL6IP1$^{L2\text{-}Myc}$), showing that the peripheral enrichment of mCh-ARL6IP1 relative to EGFP-Sec61β is impaired in the case of ARL6IP1$^{L2\text{-}Myc}$ (arrowheads). Scale bar: 5 µm. **(F)** Representative confocal images and line-scan analysis of COS-7 cells coexpressing EGFP-Sec61β and ARL6IP1^{F105E,I112E}, showing that the peripheral enrichment of mCh-ARL6IP1 relative to EGFP-Sec61β is impaired in the case of mutant ARL6IP1. Scale bar: 5 µm. **(G and H)** Representative confocal images and line-scan analysis of COS-7 cells coexpressing EGFP-tagged WT ARL6IP1 and mCh-tagged ARL6IP1^{F105E,I112E}, highlighting their different localizations. ARL6IP1$^{F105E,\ I112E}$ does not exhibit the peripheral enrichment in the tubular ER (F) and ectopically localizes in ER sheets (G). Scale bars: 5 µm.

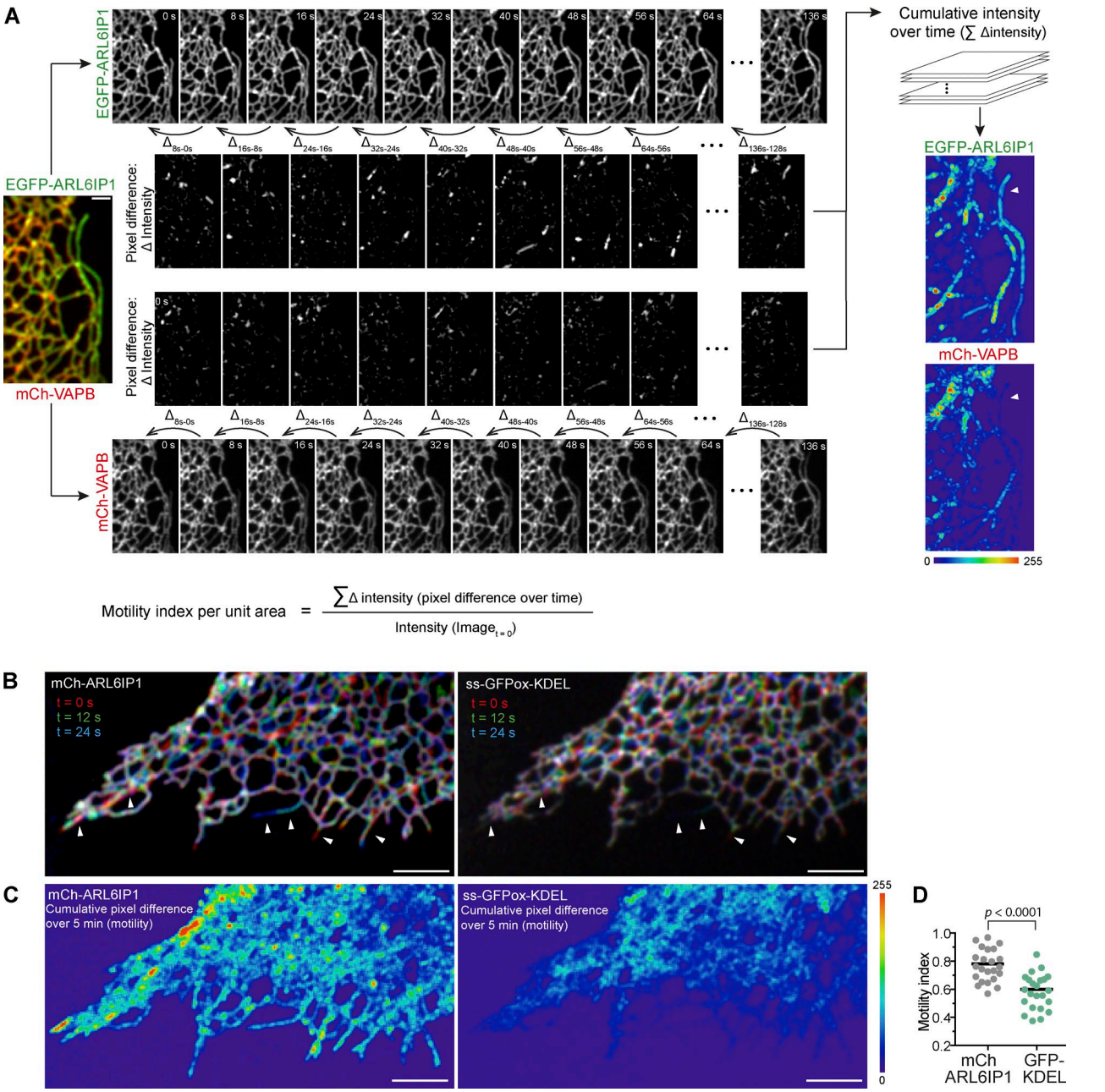

Figure S3. **Quantitative analysis of the motility of EGFP-ARL6IP1 and mCh-VAPB in the ER, demonstrating the method used for the generation of Fig. 4, A–D, and Fig. S3, B and D. (A)** Motility of ER proteins. COS-7 cells coexpressing EGFP-ARL6IP1 and mCherry (mCh)-VAPB were imaged by confocal live-cell microscopy. Scale bar: 2 µm. EGFP and mCh signals were separated into two stacks of sequential images, and differences of fluorescence intensity at each pixel between two subsequent images were calculated (Δ Intensity). The differences at each pixel were added up to generate a cumulative intensity difference (∑Δ intensity) and pseudocolored using the Physics look-up table in Fiji. These numbers are used to calculate a motility index: cumulative fluorescence intensity changes as an ER protein moves over time normalized to the initial fluorescence intensity. **(B and C)** Analysis of motility of mCh-ARL6IP1 and ss-GFPox-KDEL. COS-7 cells coexpressing EGFP-ARL6IP1 and the ER luminal marker ss-GFPox-KDEL were imaged by confocal microscopy. Images at three time points were color-coded and merged (top), so that the stationary ER elements staying on the same sets of pixels appear white, while the motile ER elements occupying alternate pixels appear in colors. Note the abundance of the colored ER tubules in ARL6IP1 images, relative to the VAPB and KDEL images (arrowheads). Scale bars: 5 µm. Bottom: Graphic display of motility from the same field shown in B during 5-min recordings. Differences in fluorescence intensity at each pixel between subsequent time-lapse images were calculated, and these values are added up and pseudocolored. **(D)** Plots of motility index for mCh-ARL6IP1 and ss-GFPox-KDEL. Data are represented as scattered dots with the solid black bar as mean. *n* = 24 cells (two-tailed *t* test).

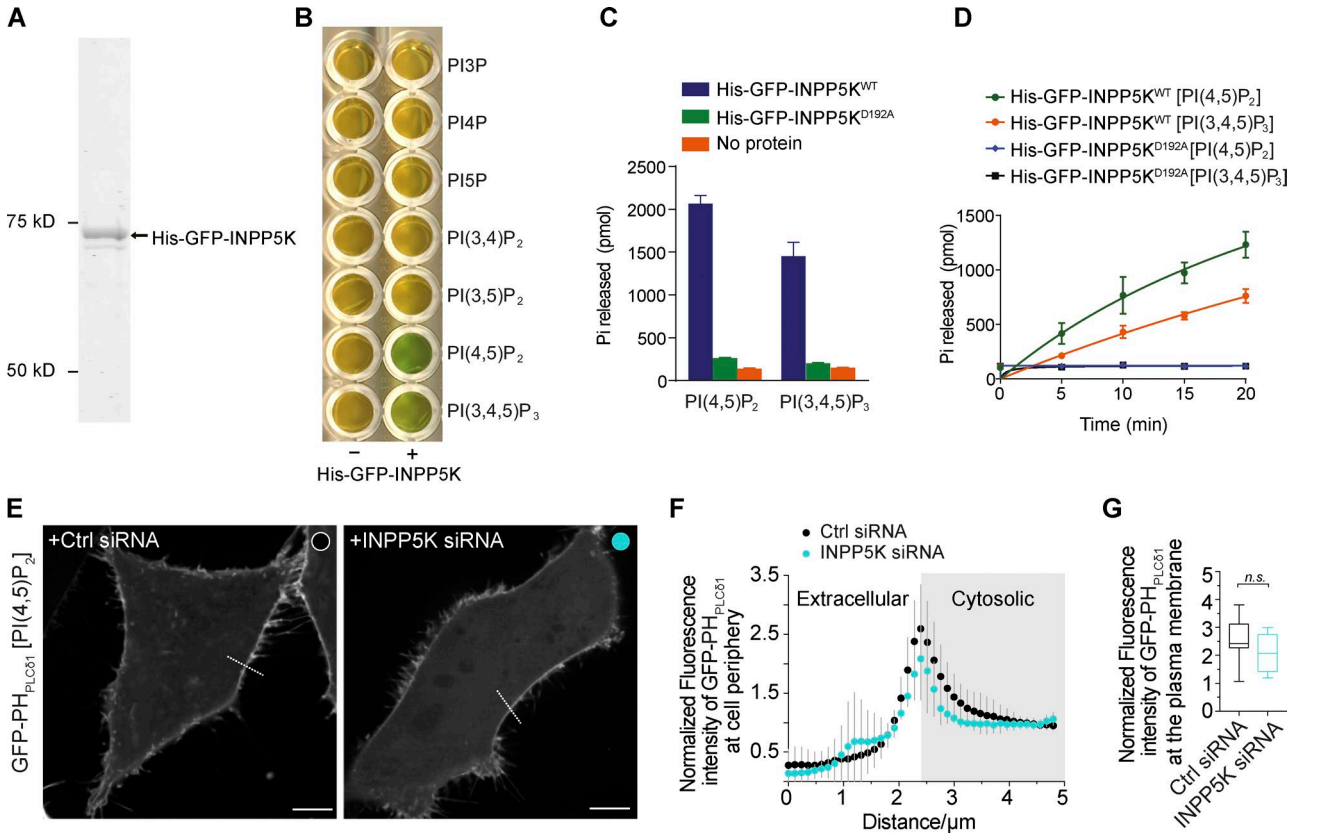

Figure S4. **Cloning, overexpression, and purification of INPP5K, INPP5K activity assay, and impact on cellular PI(4,5)P_2 distribution by the loss of INPP5K. (A)** His-GFP-INPP5K was expressed in Expi293 cells, purified by nickel resin followed by gel filtration, and analyzed by SDS-PAGE stained by Coomassie blue. **(B–D)** Phosphatidylinositide phosphatase activity assay with purified His-GFP-INPP5K and malachite green assay. Quantification of the assays shown in C and D. Data represent mean ± SD. **(E–G)** Loss of INPP5K does not result in an obvious change of cellular PI(4,5)P_2 distribution. (E) Representative confocal images of WT cells transfected with control or INPP5K siRNA and expressing the PI(4,5)P_2 probe GFP-$PH_{PLC\delta1}$, showing the enrichment of this probe in the plasma membrane and no changes between WT and INPP5K siRNA-treated cells. Scale bars: 5 µm. (F and G) Quantifications of the plasma membrane/cytosol ratio of GFP-$PH_{PLC\delta1}$ fluorescence based on line scans as exemplified in (E; mean ± SD, n = 12 cells for cells treated with control or INPP5K siRNAs; n.s., not significant by two-tailed t test).

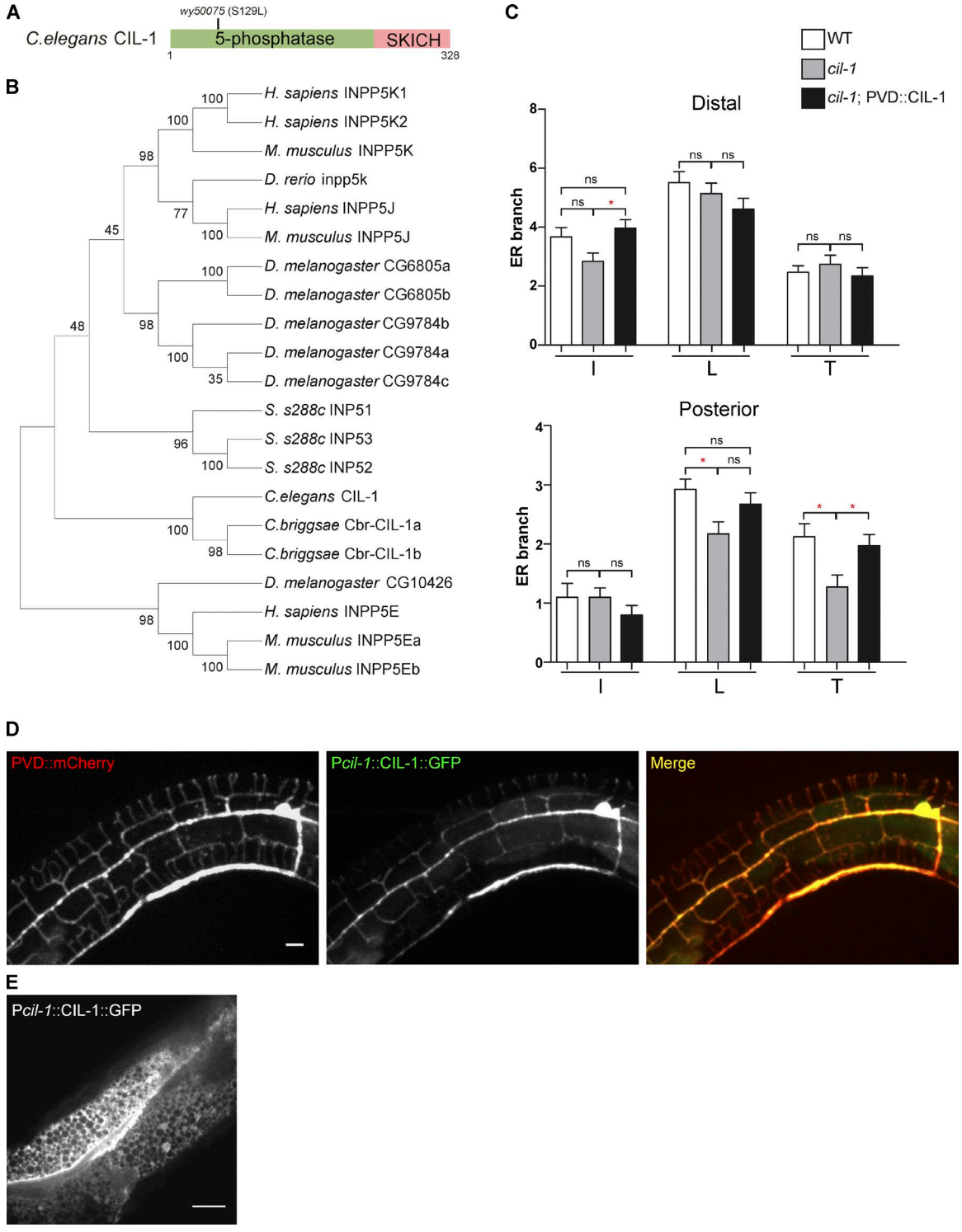

Figure S5. **Domain organization and phylogenetics of CIL-1 and endogenous expression of CIL-1 in PVD neurons. (A)** Domain structure of the CIL-1 protein and location of the point mutation in the *wy50075* allele. **(B)** A phylogenetic tree of *C. elegans* CIL-1 and its orthologues in other species. **(C)** Quantification of PVD distal and posterior regions ER branches. The quantifications are plotted. *, $p < 0.05$; ns, not significant by one-way ANOVA. Error bars indicate SEM. $n = 40$ for each genotype. **(D)** Representative confocal micrograph of a transgenic worm expressing *cil-1::cil-1::gfp* (the *cil-1* genomic fragment fused with GFP) and coexpressing PVD mCherry. Note that the PVD neuron is labeled by CIL-1::GFP. Scale bar: 10 µm. **(E)** CIL-1::GFP fluorescence is also detected in other tissues in these worms as shown here by the fluorescence of intestinal cells. Scale bar: 10 µm.

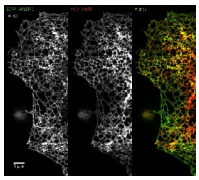

Video 1. **Live-cell confocal imaging of COS-7 cell coexpressing EGFP-ARL6IP1 and mCh-VAPB, showing the motility of ARL6IP1 relative to VAPB in the ER.** Images were acquired at a rate of one frame every 2 s for a duration of 5 min. The resulting 150 frames were displayed at 25 frames per second (playback rate is 50× real time).

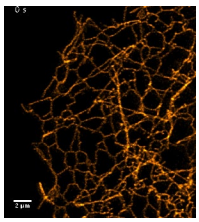

Video 2. **Live-cell nanoscopy imaging of Snap-ARL6IP1 in elongating tubules that grow along preexisting ER tubules.** Scale bar: 1 µm. Images were acquired at a rate of one frame every 2.5 s for a duration of 100 s. The resulting 40 frames were displayed at 10 frames per second (playback rate is 25× real time).

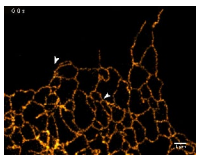

Video 3. **Live-cell nanoscopy imaging showing Halo-ARL6IP1 enriched in ER tubules exploring new territory at the periphery of the cell.** Scale bar: 2 µm. Images were acquired at a rate of one frame every 2.6 s for a duration of 39 s. The resulting 15 frames were displayed at 7 frames per second (playback rate is 17× real time).

Provided online are two tables in Excel. Table S1 lists C. elegans strains used in this study. Table S2 lists the plasmids used in this study to generate transgenic worms.